8th World Congress on Structural and Multidisciplinary Optimization
June 1-5, 2009, Lisbon, Portugal

Decision Making in Multi-Objective Optimization for Industrial Applications – Data Mining and Visualization of Pareto Data

Martin Liebscher[a], Katharina Witowski[a], Tushar Goel[b]

[a]Dynamore GmbH, Stuttgart, Germany, mal@dynamore.de
[b]Livermore Software Technology Corporation, Livermore, USA, tushar@lstc.com

1. Abstract
Data mining and visualization techniques for high dimensional data provide helpful information to substantially augment the decision making (alternative design selection) in multi-objective optimization environment. Four approaches the Parallel Coordinate Plot (PCP), the Hyper-Radial Visualization (HRV), the Self Organizing Maps (SOM), and the tradeoff plot have been implemented in [3, 1] and are evaluated in this paper by means of industrial sized examples.

2. Keywords: multi-objective optimization (MOO), parallel coordinate plot (PCP), hyper-radial visualization (HRV), self organizing maps (SOM), LS-OPT

3. Introduction
Optimization of engineering structures where multiple (more or less conflicting) objectives are simultaneously considered, is getting more and more attractive in automotive industries. They usually involve a large number of design variables and the objectives are subject to certain constraints. Unlike single-objective problems, there are many trade-off solutions.
The most common approach of using a single aggregate objective function (AOF), though simple, is not appropriate in most cases because a) it requires a priori information, e.g. weights associated with each objective for weighted linear sum of the objectives method, that might not be available; and b) this approach yields a single trade-off solution instead of all possible trade-off solutions.
Multi-objective evolutionary algorithms (MOEA) seem to be the best choice at the moment to overcome these issues. A set of solutions (Pareto data) is obtained as result, which reflect distinct trade-off solutions. A (optimal) decision needs to be taken to choose the most suitable trade-off among multiple conflicting objectives.
A graphical approach to visualize the Pareto frontier is an intuitive and suitable approach to investigate the trade-off for three or fewer dimensions (objectives). However, it is not trivial to study relations in higher dimensions hence many visualization methods are proposed. The basic idea of these techniques is to reduce the dimensionality without loosing the relevant information required to recognize and understand relations and characteristics of the high dimensional Pareto data. Among the several developments in these fields, the Parallel Coordinate Plot (PCP), the Hyper-Radial Visualization (HRV), and the Self Organizing Maps (SOM) have been found the most promising.
The parallel coordinate plot assigns one axis to each dimension and many dimensions are aligned in parallel. A data point is represented as a line connecting different axes. The HRV is based on a radial calculation and transfers the multi-dimensional data to a two-dimensional data set by grouping the weighted objectives, that leads to a final solution with respect to the selected weights and the grouping. The designer incorporates his preferences by modifying the selection. The SOM algorithm projects the multi-dimensional Pareto data onto a two-dimensional map, whereby similar data is mapped to neighboring locations on the map. The lattices are color-coded to show the variation of the data on the map.
The concepts of PCP, HRV and SOM are explained along with the various forms of visualization of Pareto data. All three approaches are investigated and respective pros and cons are identified using a few shape optimization case crash applications executed with LS-OPT. An implementation in the data mining and visualization framework D-SPEX is also provided.

4. Methodologies

4.1. Tradeoff Plot

The most intuitive way of visualizing high dimensional data is the Tradeoff plot, Figure 1. The data is projected into a three-dimensional space. A forth dimension may be visualized using the color of the points, a fifth dimension using the size.

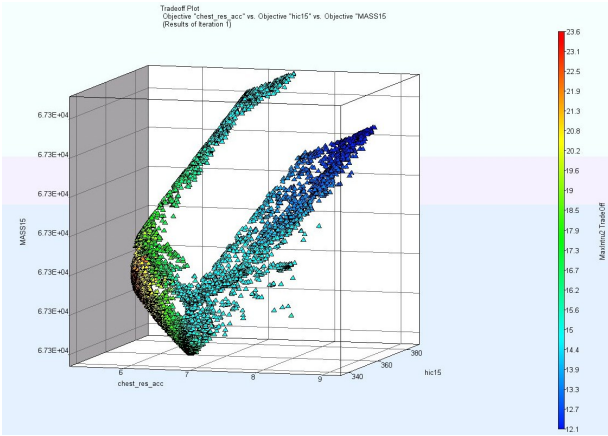

Figure 1: Tradeoff plot visualizing four dimensions

4.2. Parallel Coordinate Plot (PCP)

The Parallel Coordinate Plot visualizes each dimension on a vertical axis and each data point as a polyline connecting the respective values on the vertical axis. The number of dimensions that can be visualized using the Parallel Coordinate Plot is not restricted, but too many data points may result in a dense and unclear view. An example of PCP is displayed in Figure 11.

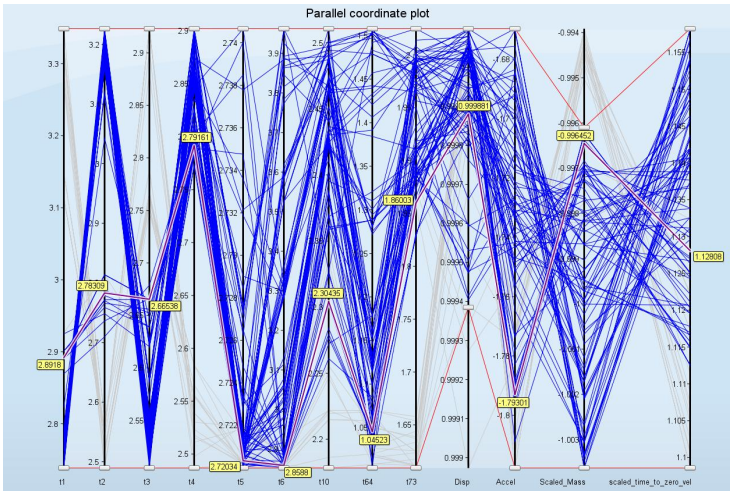

Figure 2: Parallel Coordinate Plot

4.3. Hyper-Radial Visualization (HRV)

The Hyper-Radial Visualization (HRV) maps multi-dimensional data into a two-dimensional space. The objectives are grouped and a weighted sum of each group is calculated. These values are displayed in two-dimensions. The HRV method is explained in detail below.

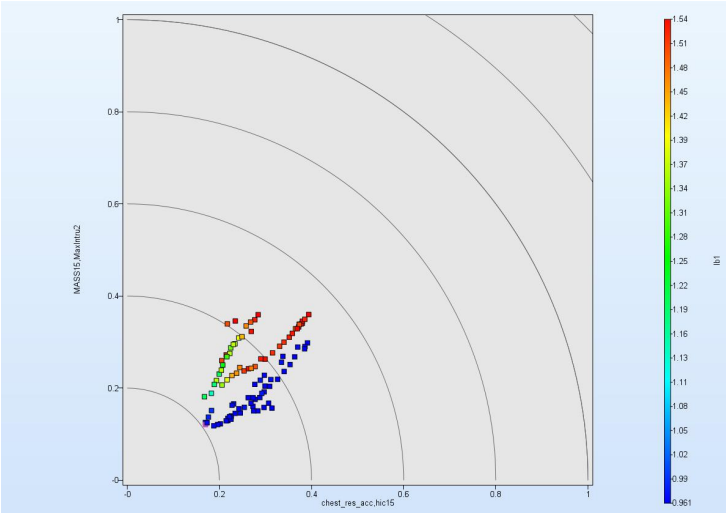

Figure 3: Hyper-Radial Visualization

Usually, the objective functions have different values and units, hence the normalization of objective values F_i is necessary to obtain meaningful results. The normalized objective values $\tilde{F}_i$ are calculated using Eq. 1,

$$\tilde{F}_i = \frac{F_i - F_{i,min}}{F_{i,max} - F_{i,min}},\ i = 1 \dots n \tag{1}$$

where n is the number of objectives, $F_{i,min}$ and $F_{i,max}$ are the minimal and maximal values of objective F_i, respectively. The next step is to group the objectives into two sets $F_1, F_2, \dots, F_s$ and $F_{s+1}, F_{s+2}, \dots, F_n$, and to calculate the weighted Hyper-Radial Calculation values HRCW1 and HRCW2

$$\begin{aligned} \text{HRCW1} &= \sqrt{\frac{\sum_{i=1}^{s} W_i \tilde{F}_1^2}{s}} \\ \text{HRCW2} &= \sqrt{\frac{\sum_{i=s+1}^{n} W_i \tilde{F}_1^2}{n-s}} \end{aligned} \tag{2}$$

with $W_i > 0; \sum_{i=1}^{n} W_i = 1$. Hence, the two-dimensional data set (HRCW1, HRCW2) represents the n-dimensional data set $(F_1, \dots, F_n)$. The engineer may incorporate his preferences by selecting larger weights for more important objectives and lower weights otherwise. In addition to the two-dimensional data set (HRCW1, HRCW2), indifference curves are displayed (Figure 12). Each point on an indifference curve has the same preference. If $n - s = s$, the indifference curves are circles around the origin. The indifference curves closer to the origin, which is the ideal point for the normalized objectives, are of greater importance. If $n - s \neq s$, dummy objective functions with all values equal to zero are added to normalize the visualization.
In the end, the point on the nearest indifference curve to the ideal point is calculated, which is the optimal solution for the selected weights. So the HRV offers a method to select a single solution out of the various Pareto optimal solutions.
For more details on the HRV, see [7].

4.4. Self Organizing Maps (SOM)
Self organizing map [9] is an unsupervised neural network algorithm that projects multi-dimensional data onto a two-dimensional array of nodes. 108 nodes are arranged on a regular 9x12 hexagonal grid. Each node is associated with a randomly initialized n-dimensional weight vector m_j, where n is the dimension of the data to be visualized, and j refers to the j^{th} node. The algorithm sorts and adapts the weight vectors such that similar data is mapped to the closest node. Each component of the weight vector may be visualized by coloring the grid according to the values of the selected component, and so many dimensions may be visualized at once by displaying several component maps side by side.

(a) initial SOM (b) trained SOM

Figure 4: initial and trained SOM

The training of a SOM is an iterative process. The weight vectors m_j are initialized randomly. At each training step t , a data point $F = [F_1, \ldots, F_n]$ from the input data set is selected and corresponding best matching unit, which is the node with the most similar weight vector m_c to the training point F is determined

$$\|F - m_c\| = \min_j \|F - m_j\| . \tag{3}$$

All weight vectors are updated as follows,

$$m_j(t+1) = m_j(t) + h_{cj}(t)(F - m_j(t)). \tag{4}$$

The neighborhood function $h_{cj}(t)$ is defined as

$$h_{cj}(t) = \alpha(t) \exp\left(-\frac{\|r_c - r_j\|}{2\sigma(t)^2}\right), \tag{5}$$

where r_j is the coordinate of node j in the two-dimensional grid, the learning rate function α is given as

$$\alpha(t) = \frac{\alpha_0}{(1 + 100\frac{t}{T})}, \ \alpha_0 = 0.9, \tag{6}$$

and the radius of influence σ varies with the time as,

$$\sigma(t) = \sigma_0 \left(1 - \frac{t}{T}\right), \ \sigma_0 = 5. \tag{7}$$

T is the total training time which is a given number of iterations [9]. The process is stopped after T iterations.
The SOM algorithm results in a sorted map, see Figure 4. Each component of the weight vector may be visualized on a component map, see Figure 5. Comparing component maps of different entities offers e.g. information on conflicting objectives and on the relation of variables and objectives. The U-Matrix displays the distance between the weight vectors of neighboring nodes. On each edge of the hexagonal lattice, a smaller hexagon colored according to the euclidean distance between the weight vectors of the respective neighboring nodes are displayed. The color range is determined by the minimal and maximal distance, respectively. The D-Matrix displays the mean value of the distances between a node and all its neighboring nodes on the original lattice. Hence the U- and D-Matrices offer additional information on the continuity of the Pareto optimal front.

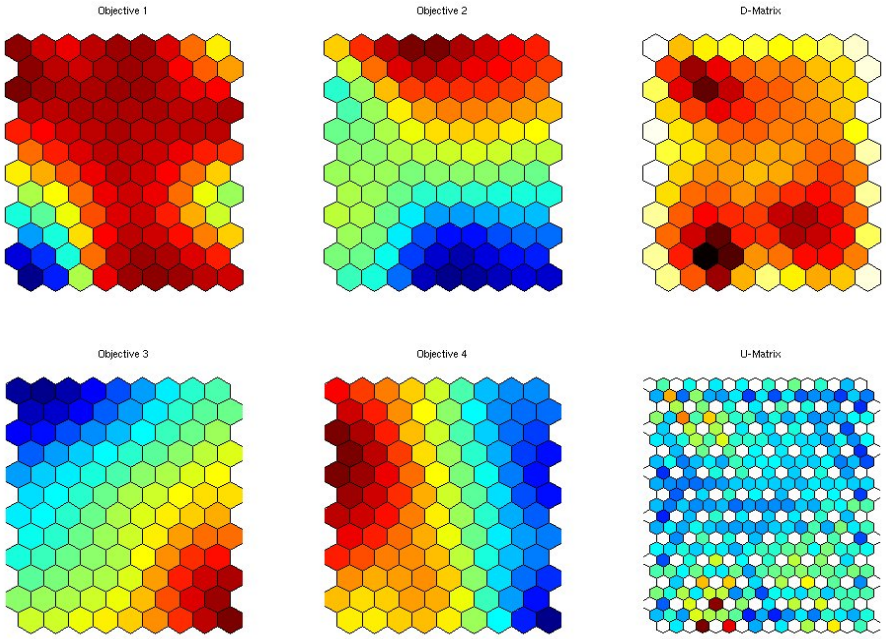

Figure 5: some component and distance maps

5. Examples

5.1. Front Crash

To demonstrate the different visualization methods for Pareto optimal solutions, a multi-objective optimization of a frontal impact of a car on a rigid barrier is considered. The finite element model obtained from [1] is displayed in Figure 6. The LS-DYNA [2] explicit solver is used to simulate the crash.

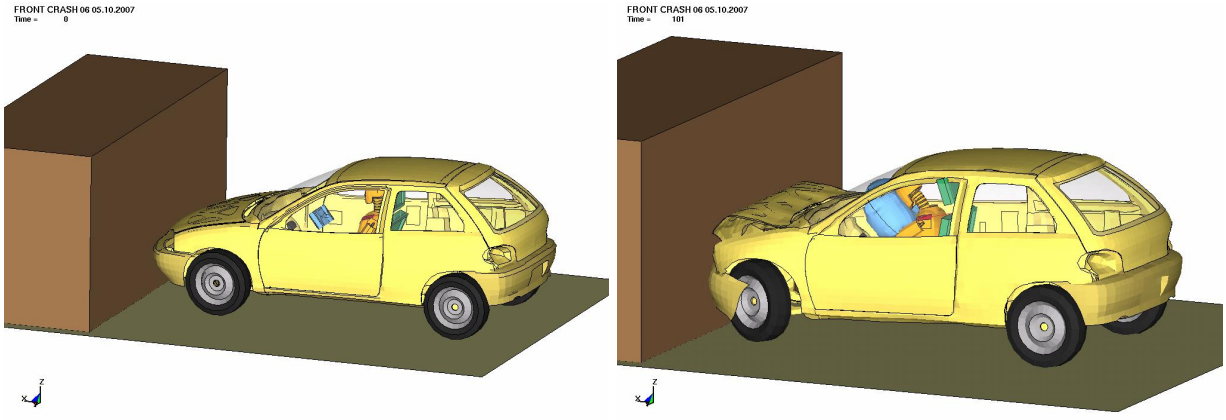

(a) t=0ms (b) t=101ms

Figure 6: Finite element crash model

The sheet thicknesses of nine parts are parametrised with six design variables, Figure 7. The initial design and the bounds on the variables are given in Table 1.

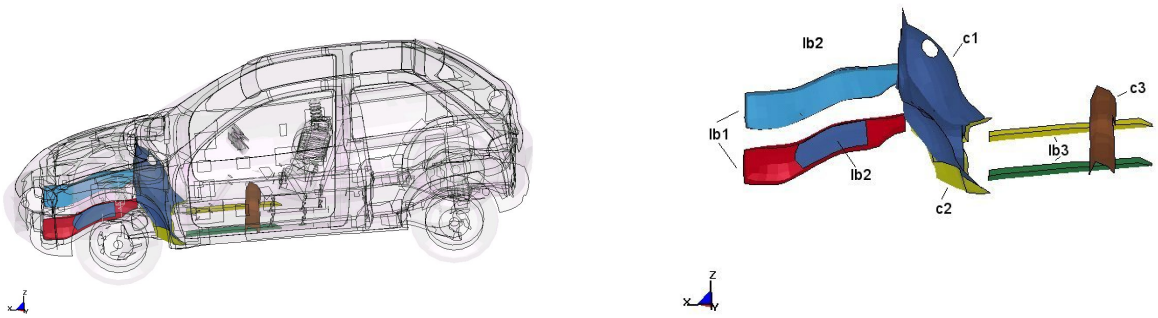

Figure 7: Design variables: sheet thicknesses of colored parts

Table 1: Design variables

Variable Description	Name	lower bound	upper bound
Rails front inner	lb1	1mm	1.5mm
Rails front outer	lb2	1.3mm	1.8mm
Rails back	lb3	0.8mm	1.3mm
Crossmember front upper	c1	0.8mm	1.3mm
Crossmember front lower	c2	0.8mm	1.3mm
Crossmember back	c3	1mm	1.5mm

The objectives considered are the chest acceleration of the dummy (chest_res_acc), the HIC value (hic15), Figure 8, the total mass of the vehicle (MASS15) and the intrusion of the cabin (MaxIntru2), Figure 9.
A meta-model based multi-objective optimization is performend with LS-OPT [3]. For all responses, RBF metamodels were constructed using 250 simulations. The elitist non-dominated sorting genetic algorithm (NSGA-II) [6] is used to find candidate Pareto optimal solutions. After evolving for 250 generations, the population of 100 individuals yielded 5942 candidate Pareto optimal solutions. This set of solutions is analyzed using the four visualization strategies.

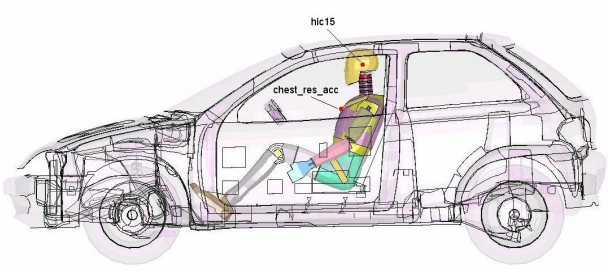

Figure 8: Objectives chest acceleration and HIC value

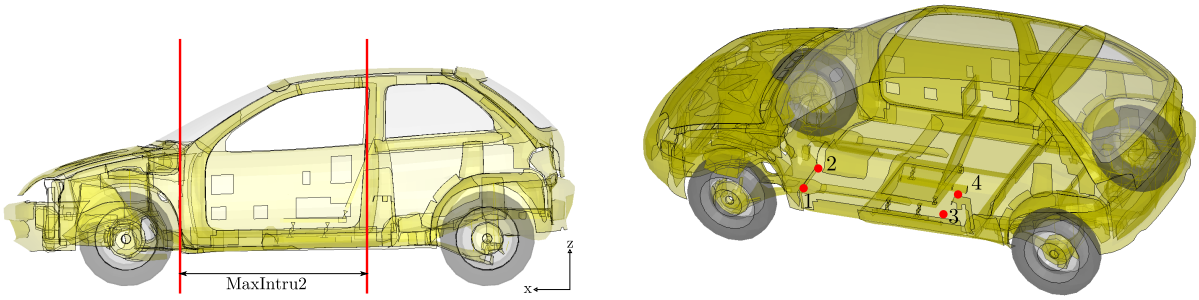

Figure 9: Objective intrusion of the cabin

5.1.1. Tradeoff Plot

The most intuitive approach to visualize the obtained data is the Tradeoff plot. In Figure 1, three objectives, chest_res_acc, hic15 and MASS15, are visualized on the axes, the fourth objective, MaxIntru2, is visualized using the color of the points.The plot demonstrates the conflict between the objectives, e.g. between the mass and the intrusion. The Tradeoff plot also provides the information of a discontinuity in the Pareto optimal front. But information on the variables is missing due to the limitation of the dimension of the presentable data.

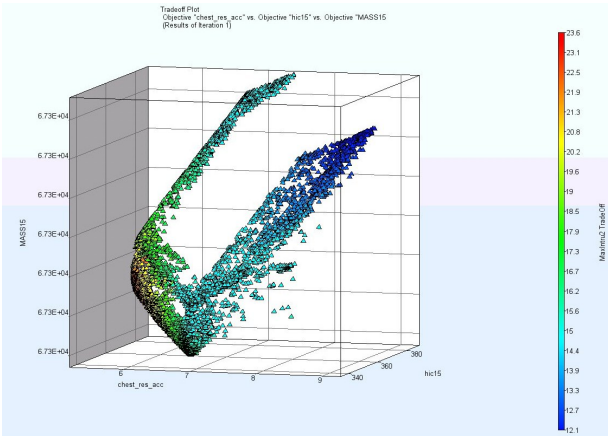

Figure 10: Tradeoff among four objectives

5.1.2 Parallel Coordinate Plot (PCP)

Figure 11 shows the parallel coordinate plot visualizing all variable and objective values. The number of dimensions to be visualized is not limited for the parallel coordinate plot, hence it is possible to add e.g. constraint values to the visualization. The engineer may easily reduce the data by adapting the ranges of all entities interactively, what is helpful in decision making. But the parallel coordinate plot offers no information on the trends.

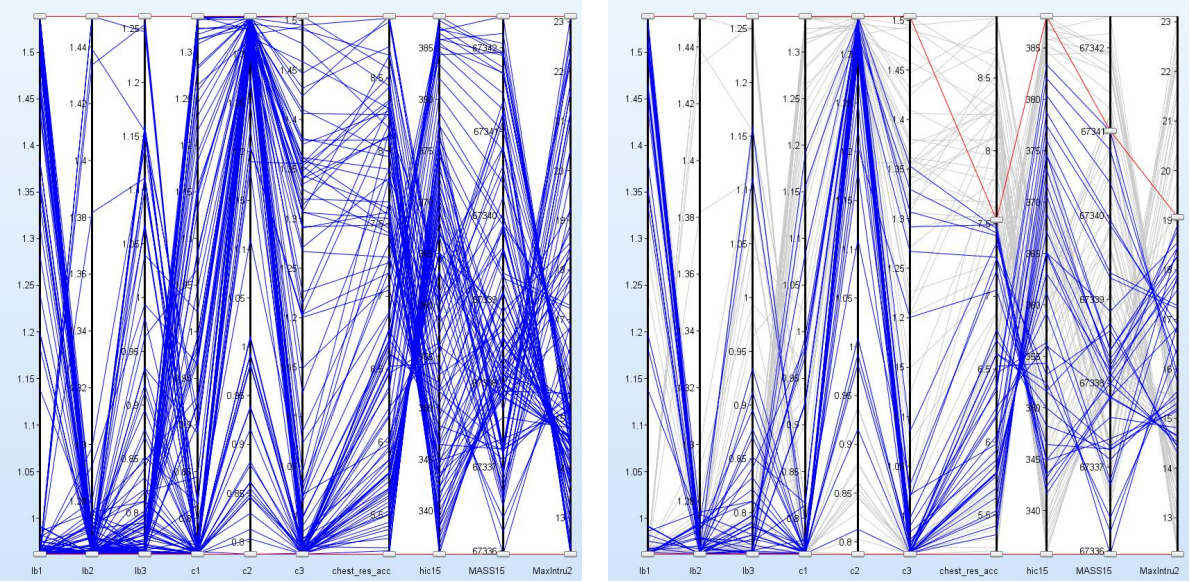

(a) original ranges (b) modified ranges

Figure 11: Paralle Coordinate Plot: variables and objectives

5.1.3 Hyper-Radial Visualization (HRV)

The hyper-radial visualization offers the possibility for the designer to incorporate his preferences by selecting weights for each objective interactively. Hence he may select larger weights for more important objectives and lower weights for the others. The objectives are grouped into two groups and a weighted sum of the objectives of the respective group is displayed in a two-dimensional plot, Figure 12. Here, chest_res_acc and hic15 are displayed on the x-axes, and MASS15 and MaxIntru2 on the y-axis. The optimal solution according to the selected weights is determined and highlighted in the plot, it is the closest point to the origin. Hence the hyper-radial visualization helps to single-out a preferred solution out of the various Pareto optimal solutions.

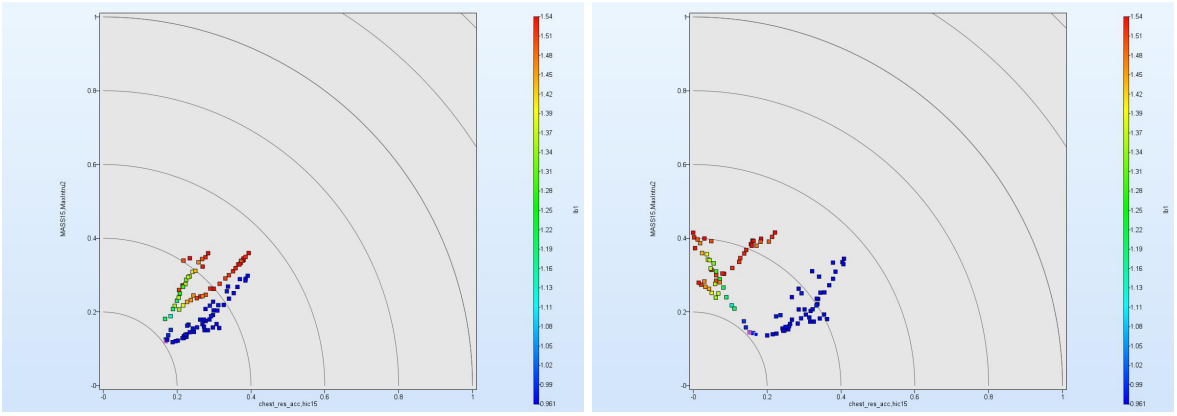

(a) equal weights for all objectives (b) weight for hic15 set to zero

Figure 12: Hyper-radial visualization

Examples for optimal designs with different preferences are given in Table 2. The first row shows the results of the objectives for the case that all objectives are treated equally, the second row shows the results for the case the weight for the objective hic15 is set to zero. That causes the worsening of hic15 and MASS15, while the other objective values are improved significantly.

Table 2: Obejective values for optimal designs with different preferences

	chest_res_acc	hic15	MASS15	MaxIntru2
equal weights	5.62	368.77	67337.3	20.5856
weight hic15 = 0	5.39	375.26	67338.6	18.19

5.1.4 Self Organizing Map (SOM)

Visualization using Self Organizing Map is a convenient tool to determine conflicting objectives and discontinuities in the Pareto optimal front. Figure 13 shows the component maps of the objectives. MaxIntru2 conflicts with all the other objectives, especially with chest_res_acc, while MASS15 and hic15 nearly have the same trend. Figure 14 shows the component maps for the variables. lb1 agrees with hic15, the values of lb2 and lb3 are largely the same for all Pareto optimal solutions, c1 correlates strongly with the MASS15 and c3 with chest_res_acc.

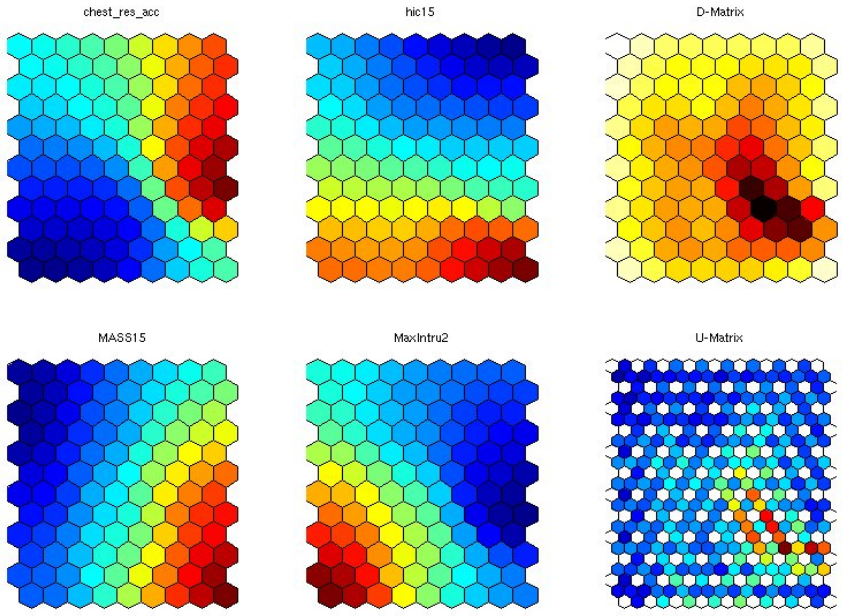

Figure 13: SOM: component maps of objectives and uniformity maps

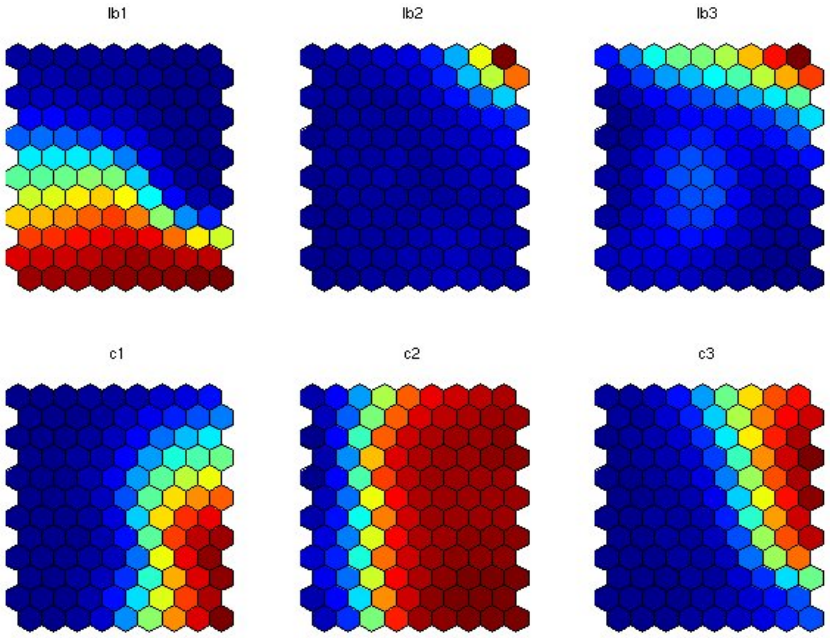

Figure 14: SOM: component maps of variables

5.1.5. Combining all visualization techniques

By plotting a combination of different plot types, one can take advantange of each method and hence get the best understanding of the Pareto optimal solutions, Figure 15. Selecting a preferred design in the HRV plot highlights the point in the parallel coordinate plot, that offers the respective information on the variable values. The Tradeoff plot holds information on the trends. Here, the best point for HRV with equal weights is marked. It is a compromise in all objectives. Most variable values for this point are near the lower bounds, one variable is near the upper bound.

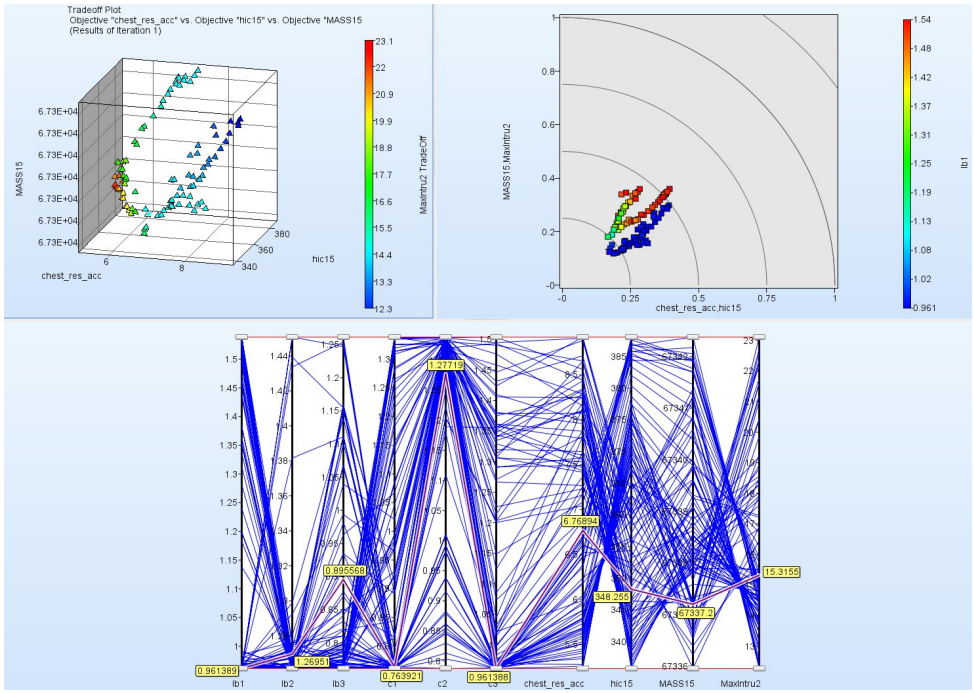

Figure 15: Tradeoff plot, HRV and parallel coordinate plot, selected point is highlighted in all plots

5.2. Truck

This optimization study is carried out by considering a crashworthiness simulation of a National Highway Transportation and Safety Association (NHTSA) vehicle undergoing a full frontal impact. The finite element model for the full vehicle, containing approximately 54,800 elements (obtained from NCAC website [1]), is shown in Figure 16. The LS-DYNA [2] explicit solver is used to simulate the crash.

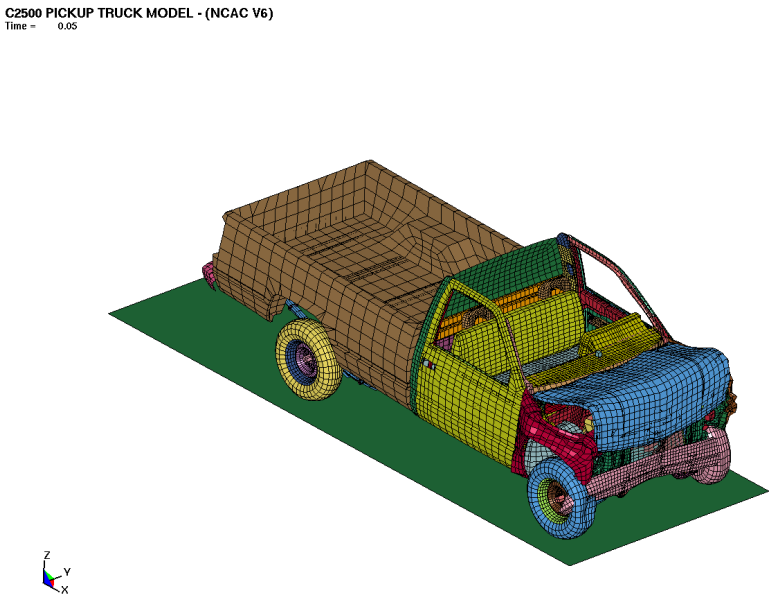

Figure 16: Finite element crash model of a pickup truck

Table 3: Baseline design and bounds on design variables

Variable description	Name	Lower bound	Baseline design	Upper bound
Rail front-right-inner	T1	2.50	3.137	3.765
Rail front-right-outer	T2	2.48	3.112	3.750
Rail front-left-inner	T3	2.40	2.997	3.600
Rail front-left-outer	T4	2.40	3.072	3.600
Rail right-back	T5	2.72	3.400	4.080
Rail left-back	T6	2.85	3.561	4.270
Bumper	T10	2.16	2.700	3.240
Radiator bottom	T64	1.00	1.262	1.510
Cabin bottom	T73	1.60	1.990	2.400

The gauges of structural components in the vehicle are parameterized directly in the solver input file. Nine gauge thicknesses associated with front-right-inner, front-right-outer, front-left-inner, front-left-outer, back-left and back-right rails, bumper, bottom-under radiator MTG, and bottom-center cabin member, are taken as design variables. The parts affected by the design variables are shown in Figure 17. The range of these design variables is chosen as within +/-20 % of the baseline design variable values. The baseline design and the bounds on the variables are given in Table 3.

Figure 17: Thickness design variables (with exploded view)

The crash performance of the vehicle is characterized by considering the maximum acceleration, maximum displacement that links to intrusion, time taken by the vehicle to reach zero velocity state, and different stage pulses. These responses are taken at the accelerometer mounted in the middle of the front seat. To reduce the influence of numerical noise, filtered acceleration is considered and different entities are averaged over two accelerometer nodes. While constraints are imposed on some of these crash performance criteria like stage pulses, it is desirable to optimize the performance with respect to other criteria. Thus a multi-objective optimization problem can be formulated as follows:

- minimize
  - mass and peak acceleration,
- maximize
  - time-to-zero-velocity and maximum displacement,
- subject to
  - the constraints on variables and performance. In this study, all objectives are minimization type and hence the optimization problem is written as
- minimize
  - mass, peak acceleration
  - -(Time-to-zero-velocity) and -(maximum displacement)
- subject to the constraints on variables and performance.

The design variable bounds are given in Table 3 and the performance constraints, namely maximum displacements and stage pulses, are specified in Table 4.

Table 4: Design constraints

	Lower bound	Upper bound
Maximum displacement (x_{crash})	-	721mm
Stage 1 pulse (x_{crash})	-	7.48g
Stage 2 pulse (x_{crash})	-	20.20g
Stage 3 pulse (x_{crash})	-	24.50g

The three stage pulses are calculated from the averaged SAE filtered (60Hz) acceleration $\ddot{x}$ and displacement x of the accelerometer nodes in the following fashion

$$\text{Stage } j \text{ pulse} = -\frac{k}{(d_2 - d_1)} \int_{d_1}^{d_2} \ddot{x} dx \tag{8}$$

with $k = 0.5$ for $j = 1$ and $k = 1.0$ otherwise.
The integration limits $(d_1; d_2) = (0; 200); (200; 400); (400; \text{Max(displacement)})$ for j = 1, 2, 3 respectively, represent different structural crash events. All displacement units are mm and the minus sign is used to convert acceleration to deceleration. All objectives and constraints are scaled to avoid dimensionality issues.
Each LS-DYNA simulation for this example problem takes approximately 3.5 hrs on Intel Xeon 2.66 GHz processor machine with 4 GB memory. Since this is a computationally intensive problem, a metamodel-based multi-objective optimization method (implemented in LS-OPT [3]) is used to obtain candidate Pareto optimal set. For all responses, the RBF metamodels were constructed using a PRESS based selection criterion as recommended by Goel and Stander [4]. A total of 997 simulation points obtained by evolving a population of 20 individuals for 50 generations (Goel et al. [3]) were used to construct metamodels.
The elitist non-dominated sorting genetic algorithm (NSGA-II) with real encoding [6] is used to find candidate Pareto optimal solutions. After evolving for 250 generations, the population of 100 individuals yielded 590 candidate Pareto optimal solutions. This set of solutions is analyzed using the four visualization strategies.

5.2.1. Tradeoff

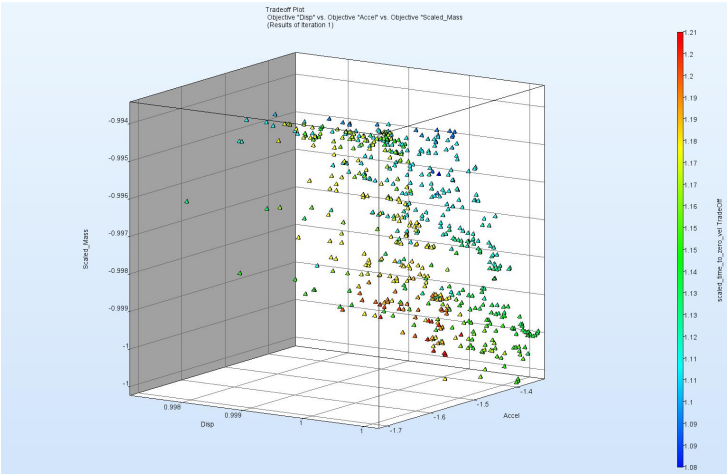

Figure 18: Trade-off among four objectives

The simple tradeoff plot (Figure 18) shows three objectives on the three axes and the fourth objective using color. One can easily visualize the conflict among objectives, infer some trade-offs like significant improvement in acceleration characteristics can be obtained by trading very small displacement. There apparently is a discontinuity in the Pareto front that might be due to the nature of the problem or just an artifact of optimization (inability to find all points). However, this graph provides limited information about the Pareto optimal front, for example, the information about the design variables and constraints is missing.

5.2.2. Paralle Coordinate Plot (PCP)
The parallel coordinate plot (Figure 19) is the simplest of all the graphs and offers more details in correlating the design variables with the responses. One can eliminate many design points by quickly changing the ranges of the variables, or objectives. Such effort helps in decision making but the most important information about the trends is missing here.

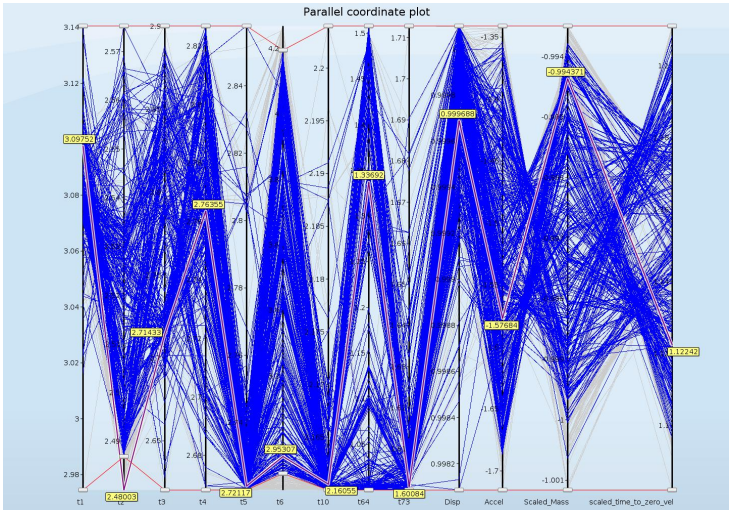

Figure 19: Parallel coordinate plot

5.2.3. Hyper Radial Visualization (HRV)
Hyper-radial visualization is a more complex way of combining the preference structure of the designer with the objectives in such a way that multi-dimensional plots are reduced to more conventional two-dimensional graphs. The most prominent feature of this plot is the ability to single-out preferred designs among all the Pareto optimal solutions. In Figure 12(a), all designs are assigned equal weight. Scaled Displacement and acceleration are plotted on the x-axis, and mass and time-to-zero-velocity are plotted on the y-axis. For this combination the best design is shown between HRV contours 0.2 and 0.3. When the weight associated with acceleration is reduced to zero, the HRV plot shown in Figure 12(b), the shape of the Pareto frontier changes significantly.

Table 5: Optimal designs with different designer preferences. All objectives are scaled values. w=1 case indicates the case when all objectives have equal weight and "no accel" case corresponds to zero weight for acceleration objective and unit weight for all other objectives.

	T1	T2	T3	T4	T5	T6	T10	T64	T73	Disp.	Accel.	Mass	Time
w=1	3.08	2.48	2.71	2.79	2.74	3.49	2.16	1.48	1.60	1.000	-1.456	-0.997	1.130
No accel.	3.10	2.49	2.78	2.78	2.72	3.03	2.16	1.01	1.60	1.000	-1.665	-0.994	1.173

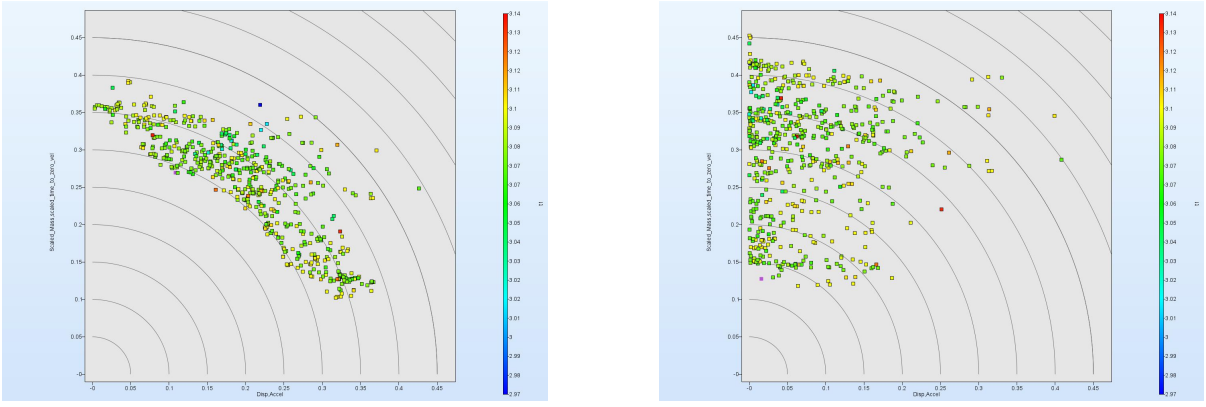

(a) equal weights to all objectives

(b) no weight to displacement objective

Figure 20: Hyper radial visualization

The best designs for the two cases are given in Table 5. One can easily see that the dropping acceleration objective significantly improves the time and mass objectives while resulting in penalties for the acceleration objective.

5.2.4. Self organizing maps (SOM)

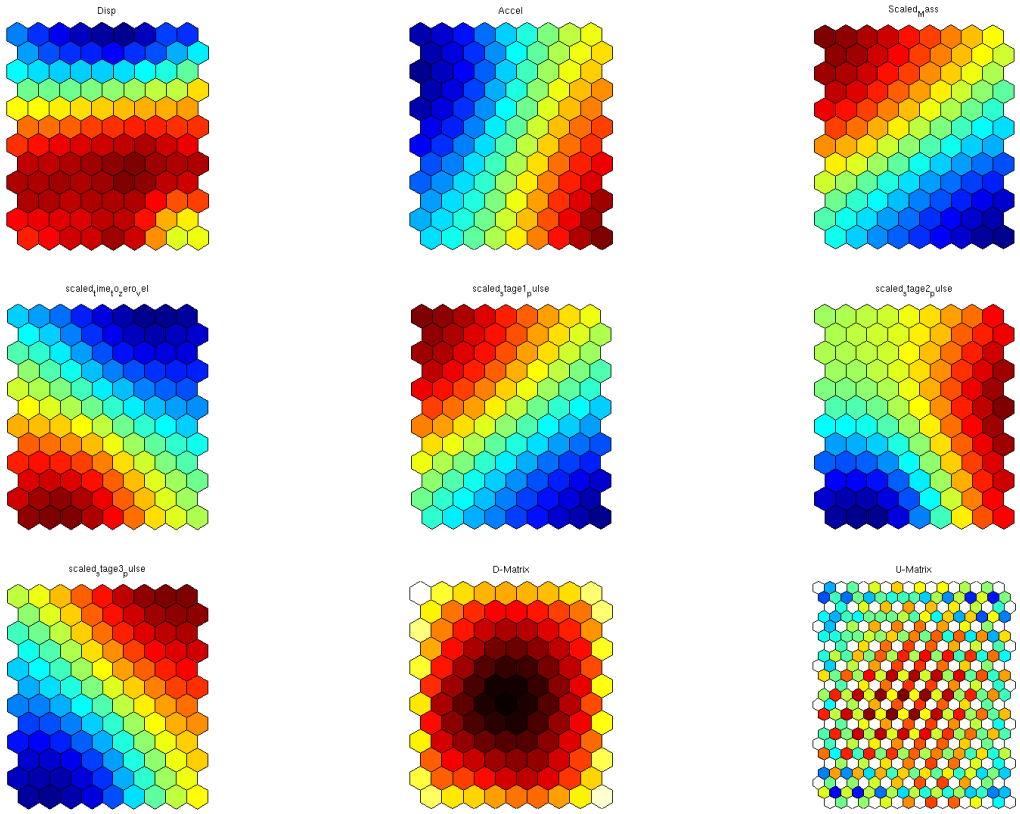

Figure 21: SOM component maps of objectives, constraints, and uniformity measures

A component map of Pareto optimal front data is plotted in Figure 21 and Figure 22. Acceleration, time-to-zero-velocity and mass are in perfect conflict. Displacement objective conflicts with other objectives but has relatively agreeable nature with the acceleration and time-to-zero-velocity. While the constraint on the first stage-pulse agrees closely with the mass, the second and third stage-pulses show conflicting behavior with all objectives. A comparative look at the design variables at the Pareto front reveal some very interesting correlations among design variables and objectives.

1. Thicknesses t2, t5, t6 and t73 are largely in agreement with the acceleration and in-inverse relation with mass and SP1.

2. Variation in the thickness t4 is in concert with the time-to-zero-velocity objective.

3. t64 correlates with stage pulse 2, t4 inversely correlates with SP3.

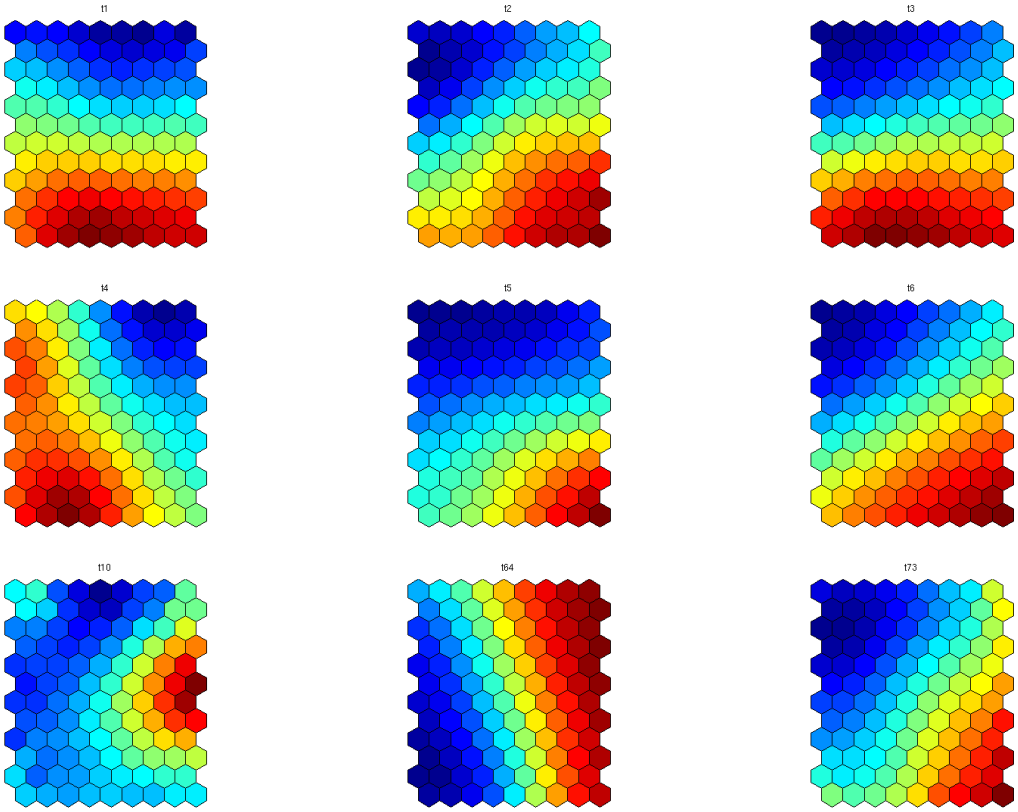

Figure 22: SOM component maps of variables at the Pareto optimal front

6. Conclusion

The decision for one or another data mining approach depends on various aspects. The first aspect is that they differ in the number of dimensions the method is capable to visualize. Another feature could be the ability to detect trends in the Pareto front, i.e. how different variables, objectives, and constraints interact in various regions. The engineer could also be interested in the continuity of the Pareto optimal front, hence the method should identify gaps in the Pareto front. In the end, the engineer needs to select a single design or a few possible designs. Does the method provide this? And last but not least, some visualization methods are more intuitive to the designer than others, and hence more comfortable to use. A recommendation based on the authors experiences is given in Tab. 6.

Table 6: Comparison of visualization methods

Feature	TradeOff	PCP	HRV	SOM
Dimensionality	best with 2/3, can display 5	any number	any number	any number
Trend analysis	weak	weak	no detection	strong detection
Discontinuities	can detect	no detection	no detection	strong detection
Design selection	weak	strong	strong	moderate
Few tradeoffs	moderate	weak	weak	strong
Ease of use	moderate	strong	strong	weak

7. References

[1] National Crash Analysis Center, http://www.ncac.gwu.edu/vml/models.html, last accessed March 11, 2009.

[2] Hallquist JO, *LS-DYNA® User's Manual*, Version 971, Livermore Software Technology Corporation.

[3] Stander N, Roux WJ, Goel T, Eggleston T, and Craig KJ, *LS-OPT® User's Manual*, Version 3.4, Livermore Software Technology Corporation, April 2008.

[4] Goel T, Stander N, *Comparing Three Error Criteria for Selecting Radial Basis Function Network Topology*, Computer Methods in Applied Mechanics and Engineering, in press (doi:10.1016/j.cma.2009.02.016).

[5] Goel T, Lin Y-Y, Stander N, *Direct Multi-objective Optimization through LS-OPT using Small Number of Crashworthiness Simulations*, 10^{th} International LS-DYNA User's Conference, Jun 8-10, Detroit MI, USA.

[6] Deb K, *Multi-Objective Optimization Using Evolutionary Algorithms*, Wiley, 2001, New York.

[7] Chiu, PW, Bloebaum, C. L., *Hyper-Radial Visualization (HRV) with Weighted Preferences for Multi-objective Decision Making*, 12^{th} AIAA/ISSMO Multidisciplinary Analysis and Optimization Conference, 2008, Victoria, British Columbia Canada.

[8] Parashar S, Pediroda V, Poloni C, *Self Organizing Maps (SOM) for Design Selection in Robust Multi-Objective Design of Aerofoil*, 46^{th} AIAA Aerospace Sciences Meeting and Exhibit, 2008, Reno, Nevada.

[9] Kohonen T, *Self-Organizing Maps*, Springer, 2001

[1] Müllerschön H. et al., *Introduction to D-SPEX*, Dynamore GmbH, Stuttgart, 2008.